

Survival of the d -Wave Superconducting State near the Edge of Antiferromagnetism in the Cuprate Phase Diagram

A. Hosseini,* D. M. Broun,† D. E. Sheehy,‡ T. P. Davis, M. Franz, W. N. Hardy, Ruixing Liang, and D. A. Bonn
Department of Physics and Astronomy, University of British Columbia, Vancouver, British Columbia, Canada V6T 1Z1

(Received 18 December 2003; published 1 September 2004)

In the cuprate superconductor $\text{YBa}_2\text{Cu}_3\text{O}_{6+x}$, hole doping in the CuO_2 layers is controlled by both oxygen content and the degree of oxygen ordering. At the composition $\text{YBa}_2\text{Cu}_3\text{O}_{6.35}$, the ordering can occur at room temperature, thereby tuning the hole doping so that the superconducting critical temperature gradually rises from 0 to 20 K. Here we exploit this to study the \hat{c} -axis penetration depth as a function of temperature and doping. The temperature dependence shows the d -wave superconductor surviving to very low doping, with no sign of another ordered phase interfering with the nodal quasiparticles. The only apparent doping dependence is a smooth decline of superfluid density as T_c decreases.

DOI: 10.1103/PhysRevLett.93.107003

PACS numbers: 74.72.Bk, 74.25.Nf, 74.62.Dh

The high temperature superconductivity puzzle has important clues in the form of ordered states of matter. One is the Mott insulator, where strong repulsion between electrons fixes them to lattice sites, with spins ordered antiferromagnetically. When doped with holes, a superconductor is encountered, one in which paired holes condense into a superfluid, but bear the stamp of the parent Mott insulator by exhibiting a d -wave symmetry favored by strong electronic repulsion. This potential for finding new states of matter drives much of the interest in systems with strong electronic correlations and in the cuprates much of this focus lies on the border between the Mott insulator and superconductor. In this regime of low hole doping, other exotic phases have been predicted [1–7], but experimentalists are hampered by a lack of homogeneous samples in which doping spans this range. Here we exploit a breakthrough [8] in the growth of high purity crystals of $\text{YBa}_2\text{Cu}_3\text{O}_{6+x}$, where doping can be continuously tuned with room temperature annealing. In the experiment presented here, the \hat{c} -axis penetration depth λ_c is measured on a sample in which critical temperature T_c is tuned from 4–20 K. Throughout this range, the temperature dependence $\lambda_c(T)$ shows that the nodal quasiparticles of the d -wave superconductor survive to very low doping, with no sign of another ordered phase interfering with their behavior. The change that does occur with doping is a smooth decline of superfluid density as the T_c is tuned down to 4 K.

A major advantage of working with the $\text{YBa}_2\text{Cu}_3\text{O}_{6+x}$ system is that the hole doping can be reversibly changed by controlling oxygen in a CuO chain layer situated 0.42 nm away from the CuO_2 planes that are the seat of the interesting physics. When the chains are completely depleted of oxygen, at $\text{YBa}_2\text{Cu}_3\text{O}_6$, the Mott insulator is encountered and when they are filled $\text{YBa}_2\text{Cu}_3\text{O}_7$ is a d -wave superconductor with a critical temperature (T_c) near 90 K. Between these extremes, Veal *et al.* [9] showed

that the loosely held dopant oxygens are mobile at room temperature and their gradual ordering into chain structures pulls electrons from the CuO_2 planes [10], increasing hole doping and T_c over time. An extreme version of this effect occurs in a narrow window of oxygen content near $\text{YBa}_2\text{Cu}_3\text{O}_{6.35}$, where crystals quenched from over 570 °C initially do not superconduct, but become superconducting with a T_c that increases with time if they are allowed to order at room temperature. This opens the door to experiments over a wide range of hole doping, all on the same crystal, with no change in cation disorder.

Here we have exploited this in a measurement of the \hat{c} -axis penetration depth, which provides information on the temperature and doping dependence of the superfluid density. A feature of the d -wave superconducting state is that the superfluid density has a linear temperature dependence due to the nodes in the energy gap, in contrast to the exponential temperature dependence coming from the uniform gap of a conventional superconductor. This linear term is seen in microwave measurements of the magnetic penetration depth λ_{ab} for superfluid screening currents flowing in the CuO_2 planes, which provide a direct measure of the superfluid density [11]. A common measurement geometry applies a microwave magnetic field parallel to the $\hat{a}\hat{b}$ plane of a crystal that is thin in the \hat{c} direction, thus avoiding large demagnetizing effects. However, this geometry includes an admixture of λ_c , the magnetic penetration depth for current flow perpendicular to the CuO_2 planes, which becomes dominant when λ_c becomes large at low hole doping. So, here we turn our focus to measuring λ_c at low doping, since $1/\lambda_c^2$ is related to superfluid density, although it is less direct because it also depends on the coupling mechanism for currents between the CuO_2 planes.

Measurements of λ_c were made in a 22.7 GHz cavity [12] with the microwave magnetic field applied along the \hat{a} axis of a crystal of $\text{YBa}_2\text{Cu}_3\text{O}_{6+x}$ [13]. The sample was

cut and polished to dimensions $(a \times b \times c) = (1.803 \times 0.203 \times 0.391 \text{ mm}^3)$ that make contributions from λ_{ab} negligible. The temperature dependence of the \hat{c} -axis penetration depth $\Delta\lambda_c(T) = \lambda_c(T) - \lambda_c(T_0)$ is extracted by measuring the shift in the cavity's resonant frequency as the sample temperature is increased above a base temperature T_0 near 1.2 K. Importantly, λ_c is large enough that the microwave fields penetrate a substantial fraction of the crystal when it is in the superconducting state, but completely penetrate the sample above T_c , making it possible to determine $\lambda_c(T_0) \simeq \lambda_c(0)$ from the frequency shift seen upon warming through T_c . A standard cavity perturbation relation $(\omega_o - \omega)/\omega_o = \Gamma[1 - 2\tilde{\delta}/d \tanh(d/2\tilde{\delta})]$ is used to extract the effective skin depth $\tilde{\delta}$ from the complex resonant frequencies ω and ω_o of the cavity with and without the sample, respectively. Γ is a geometrical constant obtained by an independent measurement on a Pb-Sn sample cut to the same dimensions as the crystal and d is the thickness. The superfluid screening length is extracted from the effective skin depth via $\lambda_c^{-2} = \text{Re}\{\tilde{\delta}^{-2}\} + \omega^2\epsilon_r/c^2$, where the term containing the \hat{c} -axis dielectric constant ϵ_r is a small contribution that displacement currents make to the screening. The value $\epsilon_r = 20$ determined by far infrared measurements [14] comes mainly from phonons and at a frequency of 22.7 GHz gives a displacement current contribution of $4.5 \times 10^6 \text{ m}^{-2}$, a correction of order 1% except for the very lowest T_c samples and very near T_c . A weak temperature dependence of Γ due to demagnetizing effects has been corrected for.

Figure 1 shows the rise of both T_c and $1/\lambda_c^2$ as the hole doping increases. The first remarkable feature of the data is the wide range of doping that can be accessed in one crystal, with T_c 's ranging from 4 to 20 K, all with sharp transitions of width 1 K. The three sets of curves indicated by squares, triangles, and circles show the results of three anneals in which the oxygen content was adjusted in a narrow range near $O_{6.35}$ by annealing between 894 and 912 °C in flowing oxygen, followed by a homogenization anneal at 570 °C in a sealed quartz ampoule with ceramic at the same oxygen content, then a quench to 0 °C. At each oxygen content the hole doping drifted up by way of oxygen ordering at room temperature, while remaining in the microwave apparatus. A noteworthy feature of the data is that the results at different oxygen contents overlap one another, indicating that for any particular T_c , the behavior of $1/\lambda_c^2(T)$ does not depend on details of the degree of chain order and oxygen content and is likely determined simply by the hole-doping level. A second feature is that at low temperatures the *absolute change* in $1/\lambda_c^2$ with temperature has almost *no* doping dependence, in contrast to the large changes in $1/\lambda_c^2(0)$ and T_c . Figure 2 focuses on this by plotting $1/\lambda_c^2(T) - 1/\lambda_c^2(0)$, which reflects the depletion of the superfluid density by quasiparticles thermally excited out of the condensate.

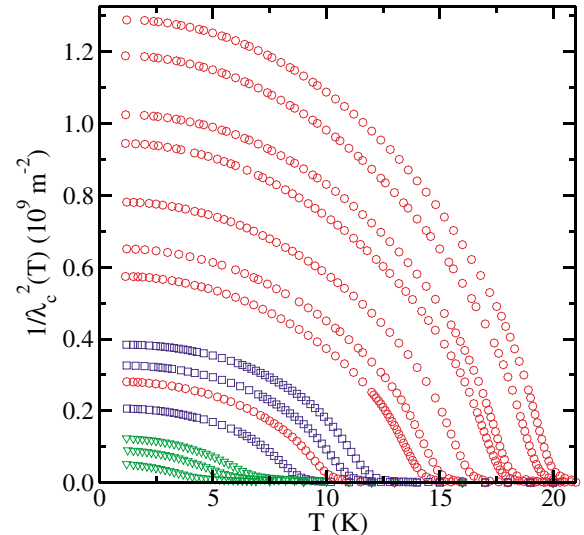


FIG. 1 (color online). Growth of critical temperature and \hat{c} -axis screening with increasing hole doping in $\text{YBa}_2\text{Cu}_3\text{O}_{6+x}$ ($x \sim 0.35$). $1/\lambda_c^2$ depends on the density of superconducting charge carriers that participate in the screening of applied fields and has been determined by a cavity perturbation measurement at microwave frequencies. The three sets of curves indicated by squares, triangles, and circles correspond to three slightly different oxygen contents and at each oxygen content the hole doping was allowed to drift up by way of gradual oxygen ordering at room temperature.

There is a collapse of the data to a power-law temperature dependence at low temperature, with little doping dependence.

Qualitatively, the first conclusion that can be drawn from the power-law behavior is that the nodes characteristic of a d -wave energy gap continue to govern the low temperature properties. If a phase transition to another state with a gap opening at the nodes had occurred, one would see the appearance of exponential rather than power-law behavior. The lack of such a change rules out transitions to other exotic superconducting states such as $d + is$ or $d + id$, which break time-reversal symmetry and open gaps at the nodes. The power law is close to $T^{2.5}$, the same as that seen in measurements of $\lambda_c(T)$ in $\text{YBa}_2\text{Cu}_3\text{O}_{6+x}$ at higher hole doping [12]. The absolute magnitude of the $T^{2.5}$ term is remarkably uniform, which suggests that the energy spectrum of the nodal quasiparticles that control the low temperature properties of the d -wave state is doping independent in this doping range. This in turn implies that the parameters that govern this spectrum, namely, the Fermi velocity v_F and the slope of the gap near the nodes, are unaffected by any other physics developing as the material approaches the limit of superconductivity in the phase diagram.

The $T^{2.5}$ power law for $1/\lambda_c^2(T)$ is different from the linear temperature dependence seen in $\lambda_{ab}^2(T)$. This near-quadratic power law has been seen in the \hat{c} -axis penetra-

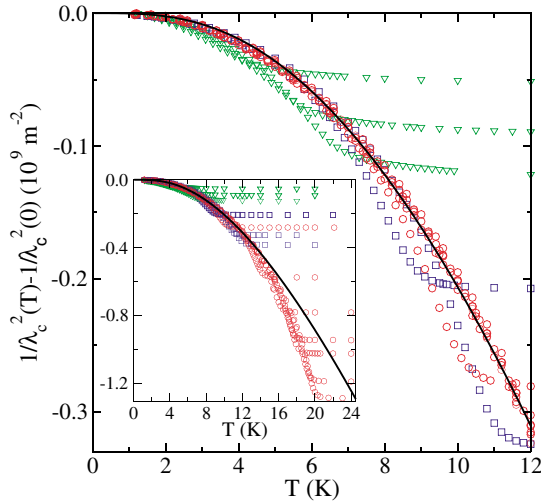


FIG. 2 (color online). A plot of $1/\lambda_c^2(T) - 1/\lambda_c^2(0)$ focuses attention on the depletion of the superfluid screening from its low temperature value, reflecting the loss of superfluid density as quasiparticles are thermally excited out of the condensate. The data for all of the doping levels shown in Fig. 1 nearly collapse onto a single curve at low T with a power law close to $T^{2.5}$. The inset shows the same data over a temperature range that spans the highest T_c . The solid curve is a fit to the low temperature data of the higher T_c samples, with a model that involves nodal quasiparticles in a d -wave superconductor, scattered as they tunnel from one CuO_2 plane to the next.

tion depth of $\text{La}_{2-x}\text{Sr}_x\text{CuO}_{4+\delta}$ [15], $\text{Bi}_2\text{Sr}_2\text{CaCu}_2\text{O}_8$ [16], and $\text{HgBa}_2\text{Ca}_2\text{Cu}_3\text{O}_{8+\delta}$ [17], as well as in $\text{YBa}_2\text{Cu}_3\text{O}_{6+x}$ at higher oxygen dopings of $x = 0.60, 0.95,$ and 0.99 [18].

Understanding this difference from the \widehat{ab} -plane behavior requires a description of how holes tunnel between CuO_2 planes. When constructing such a model, it is important to note that if the tunneling preserves the momentum of the hole and is also momentum independent, then one obtains for $1/\lambda_c^2(T)$ the linear T dependence that is seen in $1/\lambda_{ab}^2(T)$. Including scattering in the \hat{c} -axis tunneling is a natural way to obtain a nonlinear T dependence, especially in light of the very high \hat{c} -axis resistivity in these materials. The near-quadratic power law has been modeled with an anisotropic scattering mechanism for \hat{c} -axis transport [19], but recently Sheehy *et al.* have arrived at a detailed microscopic model for such a process [20]. Within this model, the T dependence starts with the nodal quasiparticles that are a defining feature of d -wave superconductors. Written in terms of vector components relative to the nodes, these quasiparticles have energy $E_p = \sqrt{p_F^2 v_F^2 + p_\Delta^2 v_\Delta^2}$, a Dirac spectrum where p_F and p_Δ are components of the quasiparticle momentum perpendicular and parallel to the Fermi surface, and the gap scale $v_\Delta = (\partial\Delta/\partial\phi)/p_F$ is the slope of the energy gap $\Delta(\phi) = \Delta_o \cos(2\phi)$ as it increases with angle ϕ away from the node. This Dirac spectrum takes the form of a

flattened cone, since v_F is known to be much greater than v_Δ [21].

Scattering is introduced as random spatial variations in the tunneling matrix element. We take the average, squared matrix element to be a Gaussian

$$\langle |t_{k-p}|^2 \rangle = \frac{t_\perp^2}{\pi\Lambda^2} \exp[-(k-p)^2/\Lambda^2] \quad (1)$$

with overall magnitude t_\perp^2 and width Λ that takes on small values so that there is only a slight change in momentum when quasiparticles tunnel from plane to plane. With this assumption, the T -dependent part of $1/\lambda_c^2$ is calculated within BCS theory for a d -wave superconductor. The solid curve in Fig. 2 shows that the model describes the temperature dependence at low temperatures well, with a single set of parameters for the scattering ($\hbar/\Lambda = 12$ nm, $t_\perp = 26$ meV) and the Dirac cone ($v_F = 3 \times 10^5$ m/s, $v_F/v_\Delta = 6.8$). A doping-independent v_F has been seen by angle-resolved photoemission (ARPES) [22], so the doping-independent v_F/v_Δ observed here implies that v_Δ does not change much through the low doping range. The key puzzle that has been solved is that the nearly quadratic temperature dependence is crossover behavior in the range $v_\Delta\Lambda < k_B T < v_F\Lambda$. At lower temperatures a higher power law dominates and at higher temperatures it is linear in T , but if $v_F/v_\Delta \gg 1$ there is a wide range where the dependence is roughly quadratic [20]. This model does not explain the T^5 power law observed in the tetragonal material $\text{HgBa}_2\text{CuO}_{4+\delta}$ (which has been attributed to momentum-dependent hopping) [17], but it does explain the power law seen in the orthorhombic cuprates [15–18].

This conventional treatment of the temperature dependence of $1/\lambda_c^2$ in terms of nodal quasiparticles completely fails to describe the doping dependence of $1/\lambda_c^2$, which varies nearly quadratically with the sample's T_c , as shown in Fig. 3. Lee and Wen [21] have noted that the superfluid density at higher doping displays a paradoxical disconnection between the slope of the linear temperature dependence, whose doping dependence is thought to be weak [18,24], and the zero-temperature value, which declines rapidly as the hole doping is reduced. The paradox lies in the fact that the zero-temperature value seems to count the small number of holes added to the Mott insulator, but the temperature dependence is consistent with a large d -wave gap on the large Fermi surface expected for a high density of electrons. Here this phenomenology is reflected in the doping-independent temperature dependence of Fig. 2 and the dramatic doping dependence of $1/\lambda_c^2(0)$ in Fig. 3. Following a suggestion by Ioffe and Millis [25], this disconnection can be modeled with an effective charge for the quasiparticles that falls to zero for states away from the vicinity of the d -wave nodes, a view inspired by ARPES measurements that show the Fermi surface restricted to small arcs of

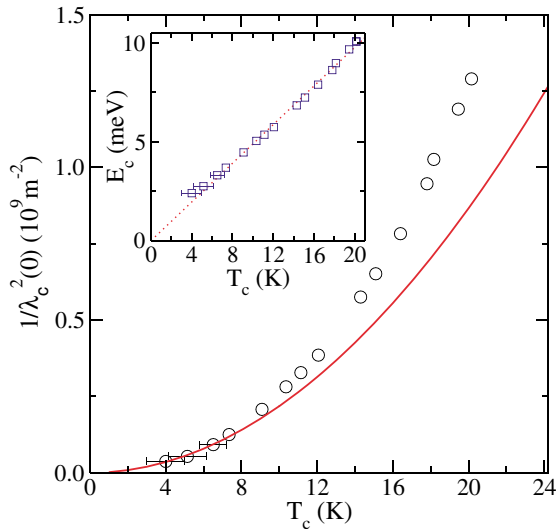


FIG. 3 (color online). Relationship between T_c and the zero-temperature value of the \hat{c} -axis screening length. The experimental correlation between these quantities (circles) can be modeled by nodal quasiparticles cut off by shrinking Fermi arcs. The inset shows the linear relationship between the cutoff energy E_c needed to model $1/\lambda_c^2$ and the measured critical temperature T_c . This model produces a nearly quadratic dependence between $1/\lambda_c^2$ and T_c , as indicated by the solid curve in the main figure. The few degree discrepancy between the T_c predicted by the model and the measured T_c is likely a consequence of phase fluctuations that govern the behavior near T_c [23].

well-defined quasiparticles when doping is decreased [26,27]. The superfluid density then comes from a truncated portion of Fermi surface [24] and Sheehy *et al.* [20] have suggested that the doping dependence can be modeled with a Dirac cone that is cut off at progressively lower energy E_c as doping is decreased. Thus the doping dependence of $1/\lambda_c^2(0)$ can be modeled with one extra parameter that is not needed in the nodal quasiparticle description of the temperature dependence. The inset in Fig. 3 displays a linearly falling E_c that is extracted from $1/\lambda_c^2(0)$ as doping and T_c decrease, indicating a superfluid density that steadily falls towards zero as T_c does. What is remarkable is that in the face of this depletion of superfluid density, the d -wave quasiparticle excitations nearest to the nodes survive and continue to govern the temperature dependence. It has recently been suggested that these nodal quasiparticles, seen here in samples with T_c as low as 4 K, even persist to dopings below the superconducting phase [22] and show up in thermal conductivity measurements in magnetic fields where T_c is driven to zero [28]. Thus the entire superconducting portion of the phase diagram, and perhaps even more, is governed by nodal quasiparticles that survive even though the Fermi surface is reduced to small arcs and the superfluid shrinks to almost nothing as the magnetism is approached.

We thank S. A. Kivelson, P. A. Lee, S.-C. Zhang, I. Herbut, C. C. Homes, and K. A. Moler for discussions. This work was supported by the Natural Science and Engineering Research Council of Canada and the Canadian Institute for Advanced Research.

*Present address: Materials Science and Engineering, Cornell University, Ithaca, NY 14853, USA.
 †Permanent address: Dept. of Physics, Simon Fraser University, Burnaby, BC, Canada V5A 1S6.
 ‡Present address: Dept. of Physics, University of Colorado, Boulder, CO 80309, USA.

- [1] P. W. Anderson, *Science* **235**, 1196 (1987).
- [2] S.-C. Zhang, *Science* **275**, 1089 (1997).
- [3] L. Balents, M. P. A. Fisher, and C. Nayak, *Int. J. Mod. Phys. B* **12**, 1033 (1998).
- [4] C. M. Varma, *Phys. Rev. Lett.* **83**, 3538 (1999).
- [5] M. Vojta, Y. Zhang, and S. Sachdev, *Phys. Rev. B* **62**, 6721 (2000).
- [6] M. Franz and Z. Tesanovic, *Phys. Rev. Lett.* **87**, 257003 (2001).
- [7] S. Chakravarty, R. B. Laughlin, D. K. Morr, and C. Nayak, *Phys. Rev. B* **63**, 094503 (2001).
- [8] Ruixing Liang *et al.*, *Physica (Amsterdam)* **383C**, 1 (2002).
- [9] B. W. Veal *et al.*, *Phys. Rev. B* **42**, 6305 (1990).
- [10] J. Zaanen, A. T. Paxton, O. Jepsen, and O. K. Andersen, *Phys. Rev. Lett.* **60**, 2685 (1988).
- [11] W. N. Hardy, D. A. Bonn, D. C. Morgan, Ruixing Liang, and Kuan Zhang, *Phys. Rev. Lett.* **70**, 3999 (1993).
- [12] A. Hosseini, S. Kamal, D. A. Bonn, Ruixing Liang, and W. N. Hardy, *Phys. Rev. Lett.* **81**, 1298 (1998).
- [13] Ruixing Liang, W. N. Hardy, and D. A. Bonn, *Physica (Amsterdam)* **304C**, 105 (1998).
- [14] C. C. Homes, T. Timusk, Ruixing Liang, D. A. Bonn, and W. N. Hardy, *Physica (Amsterdam)* **254C**, 265 (1995).
- [15] T. Shibauchi *et al.*, *Phys. Rev. Lett.* **72**, 2263 (1994).
- [16] D. M. Broun, Ph.D. thesis, Cambridge University, 2000.
- [17] C. Panagopoulos *et al.*, *Phys. Rev. Lett.* **79**, 2320 (1997).
- [18] D. A. Bonn, S. Kamal, A. Bonakdarpour, R. Liang, W. N. Hardy, C. C. Homes, D. N. Basov, and T. Timusk, *Czech. J. Phys.* **46**, 3195 (1996).
- [19] R. J. Radtke and V. N. Kostur, *Can. J. Phys.* **75**, 363 (1997).
- [20] D. E. Sheehy, T. P. Davis, and M. Franz (to be published).
- [21] Patrick A. Lee and Xiao-Gang Wen, *Phys. Rev. Lett.* **78**, 4111 (2000).
- [22] X. J. Zhou *et al.*, *Nature (London)* **423**, 398 (2003).
- [23] V. Emery and S. Kivelson, *Nature (London)* **374**, 434 (1995).
- [24] B. R. Boyce, J. A. Skinta, and T. R. Lemberger, *Physica (Amsterdam)* **341C**, 561 (1997).
- [25] L. B. Ioffe and A. J. Millis, *J. Phys. Chem. Solids* **63**, 2259 (2002).
- [26] M. R. Norman *et al.*, *Nature (London)* **392**, 157 (1998).
- [27] T. Yoshida *et al.*, *Phys. Rev. Lett.* **91**, 027001 (2003).
- [28] M. Sutherland *et al.* (to be published).